

# **Tryptophan synthase uses an atypical mechanism to achieve substrate specificity**

Andrew R. Buller, Paul van Roye, Javier Murciano-Calles, Frances H. Arnold\*

Division of Chemistry and Chemical Engineering

California Institute of Technology

Pasadena, CA 91125

**Supporting Information**

## SI Table of Contents

<b>Experimental Procedures</b> .....	S1
<b>SI Tables</b> .....	S8
<b>SI Figures</b> .....	S10
<b>References</b> .....	S11

### Experimental Procedures:

#### General

Chemicals and reagents were purchased from commercial suppliers (Sigma-Aldrich, VWR, Chem-Impex International) and used without further purification unless otherwise noted. Indole-glycerol-phosphate (IGP) was a generous gift from the Reinhard Sterner Group. Multitron shakers (Infors) were used for cell growth. Unless otherwise stated, all reactions were conducted in borosilicate glass vials (Agilent), so as to prevent to absorption of indole into plastic at elevated temperatures. UV-vis spectra were collected on a UV1800 Shimadzu spectrophotometer (Shimadzu). LC-MS data were collected on an Agilent 1290 UHPLC with a 2.1 x 50 mm C-18 silica column and a 6140 MS detector (Agilent Technologies). Samples were run using a mobile phase of water with 0.1% (v/v) acetic acid and ACN with 0.1% acetic acid. Samples were run with a linear gradient from 5-95% ACN + 0.1% acetic acid over four minutes. L-Trp eluted at 0.48 min,  $\beta$ -MeTrp eluted at 0.63 min, and indole eluted at 1.74 min.

## Cloning, expression, and purification of *Pf*TrpS, *Tm*TrpS and *Af*TrpS

The genes encoding *Pf*TrpB (UNIPROT ID Q8U093), *Pf*TrpA (UNIPROT ID Q8U094), *Tm*TrpB (UNIPROT ID P50909) and *Tm*TrpA (UNIPROT ID P50908), were previously codon-optimized for *Escherichia coli* and cloned into pET22(b)+ with a C-terminal his6-tag for the TrpBs, and without a his6-tag for the TrpAs.<sup>1, 2</sup> Briefly, a single colony of *E. coli* BL21 *E. cloni* Express cells (Lucigen) harboring the TrpA or TrpB plasmid was used to inoculate a 5-mL culture of Terrific Broth with 100 µg/mL ampicillin (TB<sub>amp</sub>) and incubated overnight at 37 °C and 250 rpm. This culture was used to inoculate a 500-mL TB<sub>amp</sub> expression culture, which was incubated at 250 rpm and 37 °C for ~ 3 h or until an OD<sub>600</sub> of 0.8 was reached. Cultures were chilled on ice for 20 min and expression was induced by the addition of 1.0 M isopropyl β-D-thiogalactopyranoside (IPTG) to a final concentration of 1 mM. Cells continued to grow shaking at 250 rpm and 20 °C for another 20 h. Cells were harvested by centrifugation at 4 °C and 5,000 g for 10 min; the pellets were frozen at -20 °C until further use.

Frozen cell pellets were thawed at room temperature and resuspended in 50 mM potassium phosphate buffer, pH 8.0, with 200 µM PLP, 1 mg/mL hen egg white lysozyme, and 0.02 mg/mL DNase. After vortexing, cells were lysed with BugBuster (Novagen) used at ½ the concentration recommended by the manufacturer. Lysates were then incubated at 75 °C for 20 min, chilled on ice, and cleared by centrifuged at 15,000 g and 4 °C for 20 min. The amount of TrpA and TrpB present in these heat-treated lysates was then estimated by SDS-PAGE, and the heteromeric TrpS complex was formed by mixing C-His-TrpB with an approximate two-fold molar excess of untagged TrpA. The resultant complex was purified by Ni-affinity chromatography on an AKTA purifier FPLC system (GE Healthcare). TrpS eluted during a linear gradient from buffer A (50 mM phosphate buffer with 20 mM imidazole and 100 mM NaCl, pH 8.0) to buffer B (same as

buffer A, but with 500 mM imidazole) at 140 mM imidazole. This procedure was used for both *PfTrpS* and *TmTrpS*.

For *AfTrpS* purification, *AfTrpB* (UNIPROT ID O28672) and *AfTrpA* (UNIPROT ID O28673) were codon-optimized for *E. coli* and cloned into pET22(b)+ and pET24(a), respectively. Expression cultures, lysis and centrifugation steps were done as described for the other homologs. After centrifugation, the supernatants of both proteins were independently injected in the AKTA purifier FPLC system for Ni-affinity chromatography. The linear gradient was the same as for *PfTrpS* and *TmTrpS*. *AfTrpB* eluted at 140 mM imidazole and *AfTrpA* at 220 mM.

All purified proteins were dialyzed against 50 mM phosphate buffer, pH 8, frozen in liquid N<sub>2</sub>, and stored at -80 °C until further use. For *AfTrpS*, a ratio 2:1 of purified *AfTrpA*:*AfTrpB* was used.

## Kinetics

$\beta$ -methyl-tryptophan ( $\beta$ -MeTrp) synthase activity of *PfTrpS* was measured by monitoring product formation in a UV1800 Shimadzu spectrophotometer (Shimadzu) at 75 °C over 1 min at 290 nm using  $\Delta\epsilon_{290} = 1.89 \text{ mM}^{-1} \text{ cm}^{-1}$  at low concentrations of indole, and by end-point initial velocity measurements for high concentrations of indole.<sup>1</sup> The assay buffer contained 200 mM potassium phosphate pH 8.0, 3  $\mu\text{M}$  *PfTrpS*, and 5  $\mu\text{M}$  PLP.

Michaelis-Menten constants ( $K_M$ ) for indole were determined using a concentration range of 5.0–0.05 mM indole with the concentration of L-threonine fixed at 25 mM. For the concentration range 0.3–0.05 mM indole, the continuous spectrophotometric assay described above was employed. A discontinuous assay was used to measure initial velocities at higher concentrations of indole. These reactions were conducted at 75 °C and 30, 60, and 120 s time points were taking

by quenching an aliquot of the reaction mixture in an equal volume of 100 % acetonitrile (ACN). Denatured protein was then cleared from these aliquots by centrifugation, and the product formation was assessed by LC-MS analysis integrating the peak heights at 277 nm, the isosbestic point in the conversion of indole to  $\beta$ -MeTrp.<sup>3</sup> This assay showed good overlap with the continuous assay for lower concentrations of indole, but was generally subject to higher experimental error (Figure S3).

The  $K_M$  value for L-threonine was determined with the concentration of indole fixed at 7 mM and the initial velocities were measured via LC-MS (as described above) for 10 concentrations of L-threonine 0.5 to 20 mM. Data were fit using an in-house non-linear least squares algorithm to the Michaelis-Menten equation implemented in MatLab. The  $k_{cat}$  for the overall reaction (Table 1) was determined from the titration of indole (above).

The deamination rates with L-serine and L-threonine were measured using a continuous spectrophotometric assay that measures production of their corresponding  $\alpha$ -ketoacids. The extinction coefficients for pyruvate and  $\alpha$ -ketobutyrate at 75 °C are  $\Delta\epsilon_{320} = 20.0 \text{ M}^{-1} \text{ cm}^{-1}$  and  $\Delta\epsilon_{320} = 21.4 \text{ M}^{-1} \text{ cm}^{-1}$ , respectively. The rates of deamination with L-serine and L-threonine were determined by monitoring the whole UV-vis spectrum (described below) every minute for 10–30 min using 10–20  $\mu\text{M}$  *PfTrpS* and 20 mM Ser or Thr and measuring  $\alpha$ -ketoacid formation at 320 nm.

### **UV-vis spectroscopy**

Spectra were collected between 550 and 250 nm on a UV1800 Shimadzu spectrophotometer (Shimadzu) using 20  $\mu\text{M}$  of enzyme in 200 mM potassium phosphate pH 8.0 in a quartz cuvette. Samples were incubated at 75 °C for > 3 min to ensure a stable temperature was reached. Stage I

of the reaction was initiated by addition of 20 mM L-threonine. The initial spectrum was measured in < 15 s to limit production of  $\alpha$ -ketobutyrate from deamination of L-threonine, and subsequent spectra were collected every minute. An example of the resultant spectrum is shown in Figure S1, which had an additional 1 mM indole added before the addition of amino acid.

### **Coupling efficiency determination**

An aqueous 200  $\mu$ L solution containing an equal concentration of IGP and L-serine or L-threonine (each reagent at either 1 or 2 mM) was prepared in 0.2 M potassium phosphate buffer pH 8.0, to which 3  $\mu$ M *PfTrpS* was added. On top of this aqueous reaction solution, 200  $\mu$ L of toluene were added, which serves to trap indole that escapes from the *PfTrpS* tunnel. Reactions proceeded for 1 h at 75  $^{\circ}$ C and were cooled on ice to slow the reaction. A 50-100  $\mu$ L aliquot of each layer was taken and diluted with an equal volume of ACN, which served to fully quench the reaction. Samples were transferred to an Eppendorf tube, pelleted at 14,000 RPM and the ratio of indole to L-Trp or  $\beta$ -MeTrp analyzed via LC-MS at 277 nm.

### **Ser-Thr specificity measurement**

The specificity for L-serine in the full catalytic cycle was determined from a 200  $\mu$ L reaction containing 6  $\mu$ M *PfTrpS*, 10  $\mu$ M *AfTrpS*, or 10  $\mu$ M *TmTrpS*, 0.135 mM IGP, 0.5 mM L-serine, 500 mM L-threonine in 0.2 M potassium phosphate buffer pH 8.0. The reaction was allowed to proceed for 1 h at 75  $^{\circ}$ C for *PfTrpS* and *TmTrpS* and at 60  $^{\circ}$ C for *AfTrpS*. Reactions were quenched with 200  $\mu$ L ACN and analyzed via LC-MS. See Table S1 for further details.

Specificity for the  $\beta$ -substitution reaction of *PfTrpS* using indole (just the  $\beta$ -subunit catalytic cycle) was measured from reactions with a 100-fold molar excess of L-threonine to L-serine in

direct competitions. Reactions were set up at three different concentrations of the substrates that maintained a constant ratio of their concentrations, as described in Table S1. Reactions were conducted with 0.2 mol % *PfTrpS* and incubated at 75 °C until all of the indole was converted into product, and the enzyme was precipitated by addition of an equal volume of ACN. The reactions were analyzed via LC-MS and the results are shown in Table S1. The results from all three conditions were combined by calculating their error-weighted average, which yields a 711-fold specificity for L-serine over L-threonine in the presence of exogenous indole.

### **Protein Crystallography**

*PfTrpB* was crystallized under previously reported conditions<sup>1</sup> and grown in sitting drops against a 1-mL reservoir of 15-25% PEG3350 and 0.1 M Na HEPES pH 7.85 with mother liquor comprised of 1.5  $\mu$ L of 8.0 mg/mL *PfTrpB* and 1.5  $\mu$ L of well solution. Enzymatically synthesized and purified  $\beta$ -MeTrp<sup>3</sup> (~1 mg) was added as a solid to pre-formed crystals and allowed to equilibrate overnight. Crystals were cryo-protected through oil immersion in Fomblin Y (Sigma) and flash frozen in liquid N<sub>2</sub> until diffraction. Diffraction data were collected remotely at the Stanford Synchrotron Radiation Laboratories on beamline 12-2. Crystals routinely diffracted at or below 2.0 Å, and the data were integrated and scaled using XDS<sup>4</sup> and AIMLESS.<sup>5</sup> A resolution cutoff of CC1/2 > 0.3 was applied along the strongest axis of diffraction.<sup>5, 6</sup> These data contributed to model quality as judged by R<sub>free</sub> in the final bin < 0.4. The structure was solved using molecular replacement with PHASER, as implemented in CCP4.<sup>7, 8</sup> The search model comprised a single monomer of *PfTrpB* (PDB ID: 5DW3) subjected to 10 cycles of geometric idealization in Refmac5 and removal of all ligands. Model building was performed in Coot<sup>9</sup> beginning with data processed at 2.4 Å, followed by subsequent

inclusion of increasingly higher resolution shells of data with relaxed geometric constraints. Refinement was performed using REFMAC5.<sup>10</sup> Restraints for the  $\beta$ -MeTrp ligand were calculated using the PRODRG online server.<sup>11</sup> The MolProbity server was used to identify rotamer flips and clashes.<sup>12</sup> After the protein, ligand, and solvent atoms were built, TLS operators were added to refinement, which resulted in substantial improvements in  $R_{\text{free}}$  for the models. Crystallographic and refinement statistics are reported in Table S2. The structure is deposited with PDB ID: 5T6M.



## Supplemental Tables:

**Table S1. Specificity of TrpS enzymes for Ser vs. Thr measured from direct competition**

Enzyme	[Ser] (mM)	[Thr] (mM)	[Indole] ( $\mu$ M)	[IGP] ( $\mu$ M)	Trp	$\beta$ -MeTrp	Specificity for Ser
<i>Pf</i> TrpS	0.5	50	300	0	397 <sup>+</sup>	55 <sup>+</sup>	723 $\pm$ 8
<i>Pf</i> TrpS	1	100	500	0	764 <sup>+</sup>	124 <sup>+</sup>	618 $\pm$ 23
<i>Pf</i> TrpS	2	200	1000	0	1,380 <sup>+</sup>	224 <sup>+</sup>	615 $\pm$ 93
<i>Pf</i> TrpS	0.5	500	0	135	175,679*	N. D.*	>82,000
<i>Tm</i> TrpS	0.5	500	0	135	136,173*	1,658*	~82,000
<i>Af</i> TrpS	0.5	500	0	135	131,599*	N. D.*	>82,000

<sup>+</sup> Integration of the absorbance peak from a trace at 277 nm.

\*Integration of the appropriate extracted [M+1] ion count detected by the MS.

N.D. = Not detected.

Activity measured using 6  $\mu$ M *Pf*TrpS, 10  $\mu$ M of *Af*TrpS or *Tm*TrpS in 0.2 M potassium phosphate buffer pH 8.0 with a 1-h reaction at 75 °C for *Pf*TrpS and *Tm*TrpS and 60 °C for *Af*TrpS. All experiments conducted in triplicate. Specificity calculated as the ratio of the Trp and  $\beta$ -MeTrp products multiplied by the molar excess of Thr. Overall specificity quoted in the text was calculated as the weighted average over all experiments conducted at different concentrations of substrates.

**Table S2. Crystallographic data collection and refinement statistics**

Protein		<i>Pf</i> TrpB
Ligand		(2 <i>S</i> ,3 <i>S</i> )- $\beta$ -methyltryptophan
<b>Data Collection</b>		
Space group		P2 <sub>1</sub> 2 <sub>1</sub> 2 <sub>1</sub>
Cell dimensions (Å)		a,b,c = 82.8, 107.7, 160.1
Cell angles		$\alpha = \beta = \gamma = 90^\circ$
Wavelength (Å)		0.9795
Beamline		SSRL 12.2
Resolution (Å)		40 – 1.8
Last Bin (Å)		(1.83 – 1.80)
No. Observations		1,778,223
Completeness (%)		99.4 (98.7)
R <sub>pin</sub> (%)		0.032(1.032)
CC(1/2)		0.999 (0.452)
I/ $\sigma$ I		12.8 (0.9)
Redundancy		13.5 (13.8)
<b>Refinement</b>		
Total no. of reflections		125,283
Total no. of atoms		12,028
Final bin (Å)		(1.85– 1.80)
R <sub>work</sub> (%)		20.4 (37.2)
R <sub>free</sub> (%)		23.8 (39.1)
Average B factor (Å <sup>2</sup> )		39.9
Ramachandran plot		97.9
Favored, %		99.8
Allowed, %		99.8
Outliers, %		0.2

Values in parenthesis are for the highest resolution shell

R<sub>merge</sub> is  $\Sigma|I_o - I| / \Sigma I_o$ , where I<sub>o</sub> is the intensity of an individual reflection, and I is the mean intensity for multiply recorded reflections

R<sub>work</sub> is  $\Sigma||F_o - F_c|| / F_o$ , where F<sub>o</sub> is an observed amplitude and F<sub>c</sub> a calculated amplitude;

R<sub>free</sub> is the same statistic calculated over a 5% subset of the data that has not been included.

Ramachandran statistics calculated by the Molprobit server.

## Supplemental Figures

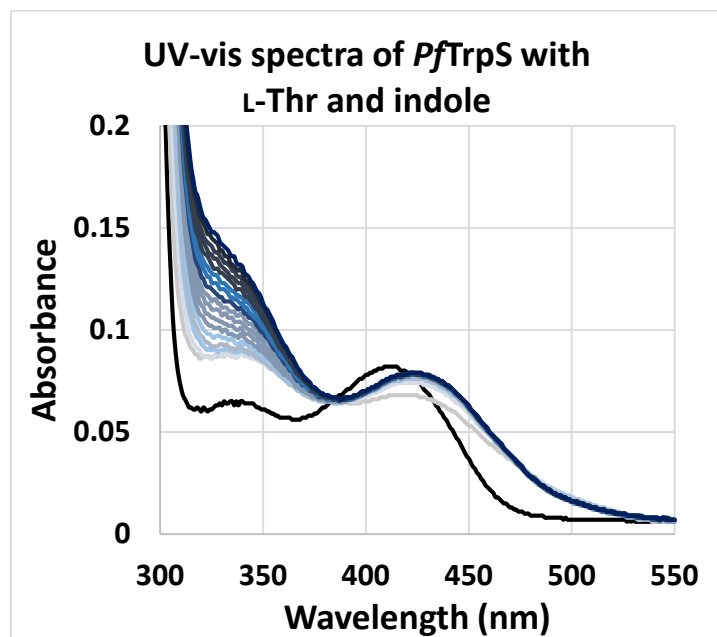


**Figure S1.** UV-vis spectra of *PfTrpS* under turnover conditions with L-Thr and indole. Incubation of 20  $\mu$ M *PfTrpS* with 1 mM indole in 0.2 M potassium phosphate buffer pH 8.0 shows the resting state of the enzyme, E(Ain), in black. Addition of 20 mM L-Thr results in a spectral shift as the enzyme reaches steady state. Spectra are colored from light gray to dark blue with one minute separating each line. This steady state reflects  $\beta$ -substitution, described in Table 1, and  $\beta$ -elimination, demonstrated by the increase in absorbance at 320 nm.

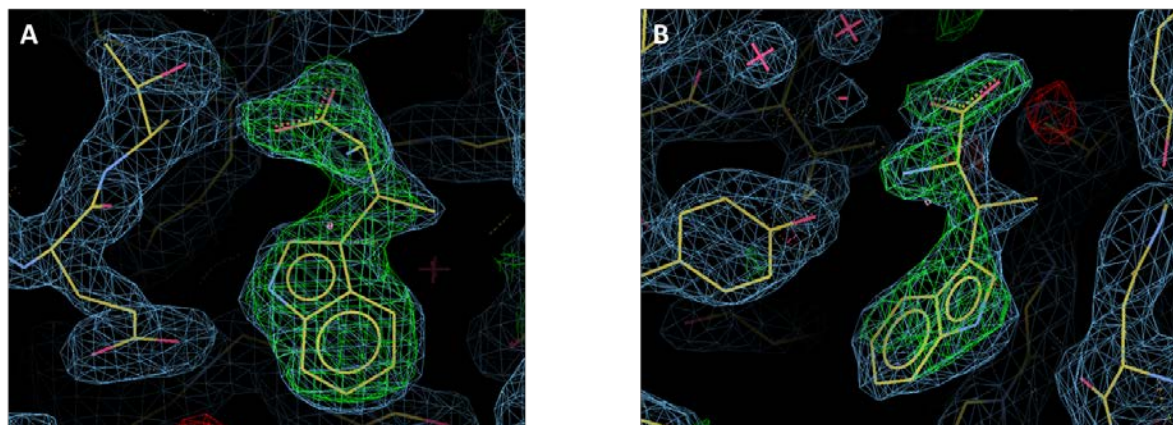


**Figure S2.** Electron density maps showing the non-covalently bound  $\beta$ -MeTrp ligand. Panel A shows  $\beta$ -MeTrp bound in the same orientation described in Figure 3A. The 2mFo-DFc map (blue) is contoured at 1.5  $\sigma$  and the mFo-DFc omit map (green = positive density, red = negative density) calculated from a model where the ligand was never included is contoured at 4.0  $\sigma$ . Panel B shows  $\beta$ -MeTrp bound in the same orientation described in Figure 3B. This ligand is

likely bound at incomplete occupancy, as indicated by the weaker density. The 2mFo-DFc map is contoured at 1.0  $\sigma$  and the mFo-DFc omit map is contoured at 3.0  $\sigma$ .

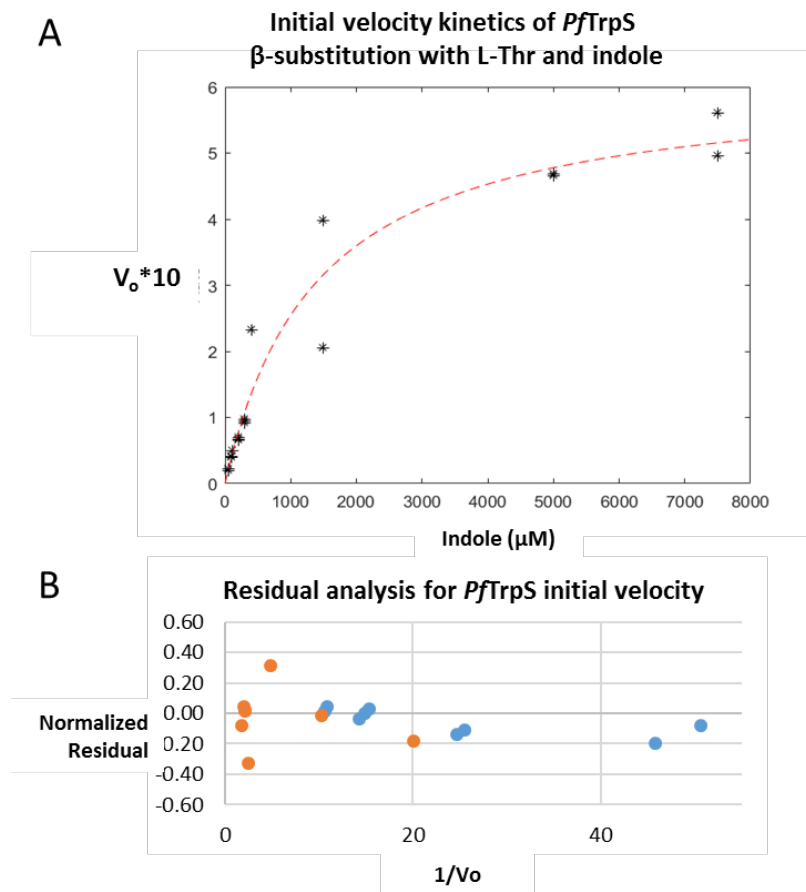


**Figure S3.** Determination of the Michaelis-Menten parameters for  $\beta$ -substitution of Thr with indole. The initial velocity kinetics of *PfTrpS* (A) were fit to the Michaelis-Menten equation using an in-house non-linear least squared fitting procedure. Data were collected by two techniques (spectrophotometric, blue; end-point, orange) and the normalized residual ( $V_{\text{obs}} - V_{\text{calc}}/V_{\text{calc}}$ ), in panel B demonstrates that end-point assay is subject to more error, but that the data generally merge well.

## References

1. Buller, A. R.; Brinkmann-Chen, S.; Romney, D. K.; Herger, M.; Murciano-Calles, J.; Arnold, F. H., Directed evolution of the tryptophan synthase beta-subunit for stand-alone function recapitulates allosteric activation. *Proceedings of the National Academy of Sciences of the United States of America* **2015**, *112* (47), 14599-14604.

2. Murciano-Calles, J.; Romney, D. K.; Brinkmann-Chen, S.; Buller, A. R.; Arnold, F. H., A Panel of TrpB biocatalysts Derived from Tryptophan Synthase through the Transfer of Mutations that Mimic Allosteric Activation. *Angewandte Chemie International Edition* **2016**, *55* (38), 11577-11581.
3. Herger, M.; van Roye, P.; Romney, D. K.; Brinkmann-Chen, S.; Buller, A. R.; Arnold, F. H., Synthesis of beta-Branched Tryptophan Analogues Using an Engineered Subunit of Tryptophan Synthase. *Journal of the American Chemical Society* **2016**, *138* (27), 8388-8391.
4. Kabsch, W., XDS. *Acta Crystallographica Section D-Biological Crystallography* **2010**, *66*, 125-132.
5. Evans, P. R.; Murshudov, G. N., How good are my data and what is the resolution? *Acta Crystallographica Section D-Biological Crystallography* **2013**, *69*, 1204-1214.
6. Karplus, P. A.; Diederichs, K., Linking Crystallographic Model and Data Quality. *Science* **2012**, *336* (6084), 1030-1033.
7. McCoy, A. J.; Grosse-Kunstleve, R. W.; Adams, P. D.; Winn, M. D.; Storoni, L. C.; Read, R. J., Phaser crystallographic software. *Journal of Applied Crystallography* **2007**, *40*, 658-674.
8. Winn, M. D.; Ballard, C. C.; Cowtan, K. D.; Dodson, E. J.; Emsley, P.; Evans, P. R.; Keegan, R. M.; Krissinel, E. B.; Leslie, A. G. W.; McCoy, A.; McNicholas, S. J.; Murshudov, G. N.; Pannu, N. S.; Potterton, E. A.; Powell, H. R.; Read, R. J.; Vagin, A.; Wilson, K. S., Overview of the CCP4 suite and current developments. *Acta Crystallographica Section D-Biological Crystallography* **2011**, *67*, 235-242.
9. Emsley, P.; Cowtan, K., Coot: model-building tools for molecular graphics. *Acta Crystallographica Section D-Biological Crystallography* **2004**, *60*, 2126-2132.
10. Winn, M. D.; Murshudov, G. N.; Papiz, M. Z., Macromolecular TLS refinement in REFMAC at moderate resolutions. *Macromolecular Crystallography, Pt D* **2003**, *374*, 300-321.
11. Schuttelkopf, A. W.; van Aalten, D. M. F., PRODRG: a tool for high-throughput crystallography of protein-ligand complexes. *Acta Crystallographica Section D-Biological Crystallography* **2004**, *60*, 1355-1363.
12. Chen, V. B.; Arendall, W. B., III; Headd, J. J.; Keedy, D. A.; Immormino, R. M.; Kapral, G. J.; Murray, L. W.; Richardson, J. S.; Richardson, D. C., MolProbity: all-atom structure validation for macromolecular crystallography. *Acta Crystallographica Section D-Biological Crystallography* **2010**, *66*, 12-21.